A reverse genetics and genomics approach to gene paralog function and disease: Myokymia and the juxtaparanode

Graphical abstract

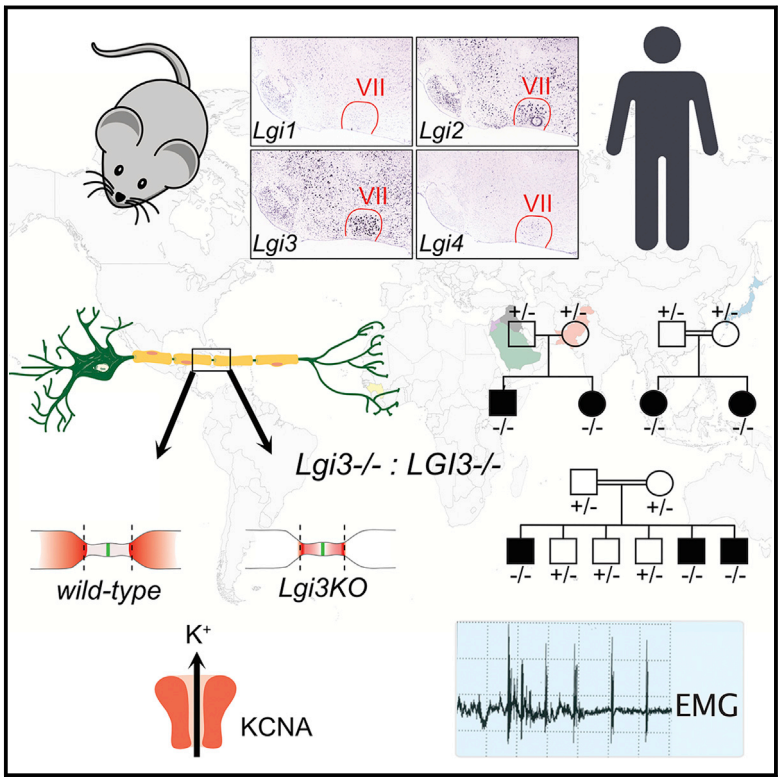

Authors

Dana Marafi, Nina Kozar, Ruizhi Duan, ..., James R. Lupski, Dies Meijer, Matias Wagner

Correspondence

jlupski@bcm.edu (J.R.L.), dies.meijer@ed.ac.uk (D.M.)

Through the power of human paralog gene studies, worldwide family-based genomics analyses, and mouse studies, we define a potentially-recognizable peripheral hyperexcitability syndrome in 16 individuals with bi-allelic *LGI3* variants and show that LGI3 co-localizes with juxta-paranodal voltage-gated potassium channels and its loss results in mis-localization of potassium channel complexes.

Marafi et al., 2022, The American Journal of Human Genetics *109*, 1713–1723
September 1, 2022 © 2022
https://doi.org/10.1016/j.ajhg.2022.07.006

A reverse genetics and genomics approach to gene paralog function and disease: Myokymia and the juxtaparanode

Dana Marafi,[1,2,36] Nina Kozar,[3,36] Ruizhi Duan,[2] Stephen Bradley,[3] Kenji Yokochi,[4,5] Fuad Al Mutairi,[6,7] Nebal Waill Saadi,[8,9] Sandra Whalen,[10] Theresa Brunet,[11,12] Urania Kotzaeridou,[13] Daniela Choukair,[14] Boris Keren,[15] Caroline Nava,[15] Mitsuhiro Kato,[16] Hiroshi Arai,[17] Tawfiq Froukh,[18] Eissa Ali Faqeih,[19] Ali M. AlAsmari,[19] Mohammed M. Saleh,[19] Filippo Pinto e Vairo,[20,21] Pavel N. Pichurin,[21] Eric W. Klee,[20,21,22] Christopher T. Schmitz,[23] Christopher M. Grochowski,[2] Tadahiro Mitani,[2,34] Isabella Herman,[2,24,25,35] Daniel G. Calame,[2,24,25] Jawid M. Fatih,[2] Haowei Du,[2] Zeynep Coban-Akdemir,[2,26] Davut Pehlivan,[2,24,25] Shalini N. Jhangiani,[27] Richard A. Gibbs,[2,27] Satoko Miyatake,[28,29] Naomichi Matsumoto,[28] Laura J. Wagstaff,[33] Jennifer E. Posey,[2] James R. Lupski,[2,25,27,30,37,*] Dies Meijer,[3,37,*] and Matias Wagner[31,32,37]

Summary

The leucine-rich glioma-inactivated (LGI) family consists of four highly conserved paralogous genes, *LGI1-4*, that are highly expressed in mammalian central and/or peripheral nervous systems. LGI1 antibodies are detected in subjects with autoimmune limbic encephalitis and peripheral nerve hyperexcitability syndromes (PNHSs) such as Isaacs and Morvan syndromes. Pathogenic variations of *LGI1* and *LGI4* are associated with neurological disorders as disease traits including familial temporal lobe epilepsy and neurogenic arthrogryposis multiplex congenita 1 with myelin defects, respectively. No human disease has been reported associated with either *LGI2* or *LGI3*. We implemented exome sequencing and family-based genomics to identify individuals with deleterious variants in *LGI3* and utilized GeneMatcher to connect practitioners and researchers worldwide to investigate the clinical and electrophysiological phenotype in affected subjects. We also generated *Lgi3*-null mice and performed peripheral nerve dissection and immunohistochemistry to examine the juxtaparanode LGI3 microarchitecture. As a result, we identified 16 individuals from eight unrelated families with loss-of-function (LoF) bi-allelic variants in *LGI3*. Deep phenotypic characterization showed *LGI3* LoF causes a potentially clinically recognizable PNHS trait characterized by global developmental delay, intellectual disability, distal deformities with diminished reflexes, visible facial myokymia, and distinctive electromyographic features suggestive of motor nerve instability. *Lgi3*-null mice showed reduced and mis-localized Kv1 channel complexes in myelinated peripheral axons. Our data demonstrate bi-allelic LoF variants in *LGI3* cause a clinically distinguishable disease trait of PNHS, most likely caused by disturbed Kv1 channel distribution in the absence of LGI3.

[1]Department of Pediatrics, Faculty of Medicine, Kuwait University, P.O. Box 24923, Safat 13110, Kuwait; [2]Department of Molecular and Human Genetics, Baylor College of Medicine, Houston, TX 77030, USA; [3]Centre for Discovery Brain Sciences, University of Edinburgh, Edinburgh, UK; [4]Department of Pediatrics, Toyohashi Municipal Hospital, Toyohashi, Aichi 441-8570, Japan; [5]Department of Pediatrics, Seirei Mikatahara General Hospital, Shizuoka 433-8558, Japan; [6]Genetics and Precision Medicine Department, King Abdullah Specialized Children's Hospital, King Abdulaziz Medical City, Ministry of National Guard Health Affairs, P.O. Box 22490, Riyadh 11426, Kingdom of Saudi Arabia; [7]King Abdullah International Research Center, King Saud Bin Abdulaziz University for Health Sciences, Ministry of National Guard Health Affairs, Riyadh, Kingdom of Saudi Arabia; [8]College of Medicine, University of Baghdad, Baghdad 10001, Iraq; [9]Children Welfare Teaching Hospital, Medical City Complex, Baghdad 10001, Iraq; [10]UF de Génétique Clinique et Centre de Reference Anomalies du Développement et Syndromes Malformatifs, APHP, Sorbonne Université, Hôpital Trousseau, 75005 Paris, France; [11]Institute of Human Genetics, Faculty of Medicine, Technical University Munich, Munich, Germany; [12]Institute of Human Genetics, Helmholtz Zentrum München, Neuherberg, Germany; [13]Division of Child Neurology and Inherited Metabolic Diseases, Centre for Pediatrics and Adolescent Medicine, University Hospital Heidelberg, Heidelberg, Germany; [14]Division of Pediatric Endocrinology, Centre for Pediatrics and Adolescent Medicine, University Hospital Heidelberg, Heidelberg, Germany; [15]Département de Génétique, Hôpital Pitié-Salpêtrière, Assistance Publique - Hôpitaux de Paris, Paris 75013, France; [16]Department of Pediatrics, Showa University School of Medicine, Tokyo 142-8666, Japan; [17]Department of Pediatric Neurology, Bobath Memorial Hospital, Osaka 536-0023, Japan; [18]Department of Biotechnology and Genetic Engineering, Philadelphia University, Amman, Jordan; [19]Section of Medical Genetics, King Fahad Medical City, Children's Specialist Hospital, Riyadh, Saudi Arabia; [20]Center for Individualized Medicine, Mayo Clinic, Rochester, MN, USA; [21]Department of Clinical Genomics, Mayo Clinic, Rochester, MN, USA; [22]Department of Quantitative Health Sciences, Mayo Clinic, Rochester, MN, USA; [23]Department of Biochemistry and Molecular Biology, Mayo Clinic, Rochester, MN, USA; [24]Section of Pediatric Neurology and Developmental Neuroscience, Department of Pediatrics, Baylor College of Medicine, Houston, TX 77030, USA; [25]Texas Children's Hospital, Houston, TX 77030, USA; [26]Human Genetics Center, Department of Epidemiology, Human Genetics, and Environmental Sciences, School of Public Health, The University of Texas Health Science Center at Houston, Houston, TX, USA; [27]Human Genome Sequencing Center, Baylor College of Medicine, Houston, TX 77030, USA; [28]Department of Human Genetics, Yokohama City University Graduate School of Medicine, Yokohama, Kanagawa 236-0004, Japan; [29]Clinical Genetics Department, Yokohama City University Hospital, Yokohama, Kanagawa 236-0004, Japan; [30]Department of Pediatrics, Baylor College of Medicine, Houston, TX 77030, USA; [31]Institute for Neurogenomics, Helmholtz Zentrum München, Neuherberg, Germany; [32]Institute of Human Genetics, Technical University Munich, Munich, Germany; [33]Centre for Regenerative Medicine, Institute for Regeneration and Repair, University of Edinburgh, Edinburgh, UK
[34]Present address: Department of Pediatrics, Jichi Medical University, 3311-1 Yakushiji, Shimotsuke, Tochigi, 329-0498, Japan
[35]Present address: Department of Neurosciences, Boys Town National Research Hospital, Boys Town, NE 68010, USA
[36]These authors contributed equally
[37]These authors contributed equally
*Correspondence: jlupski@bcm.edu (J.R.L.), dies.meijer@ed.ac.uk (D.M.)
https://doi.org/10.1016/j.ajhg.2022.07.006.

The leucine-rich glioma-inactivated (LGI) family consists of four highly homologous proteins, LGI1-4, composed of two repeat domains: N-terminal cysteine-flanked leucine-rich repeats (LRRs) and C-terminal epitempin (EPTP) repeats.[1,2] These repeats exhibit 60%–70% similarity in their amino acid sequence and highly similar domain structures, categorizing LGI1-4 within the large LRR and EPTP superfamilies.[2]

Members of the EPTP superfamily have been proposed as candidates for epilepsy and neurological disorders.[2] *LGI1-4* paralogues are highly expressed in the central and/or peripheral nervous system (CNS and PNS, respectively).[3,4] LGI3 is widely expressed in the mammalian brain,[3] where it co-localizes and interacts with endocytosis-associated proteins and SYNTAXIN-1, potentially regulating neuronal endocytosis and exocytosis.[5,6] *LGI3* expression increases dramatically during postnatal brain development, suggesting a role in neuronal differentiation, maturation, synaptogenesis, and plasticity.[7] *LGI3* is highly expressed in sensory and motor neurons in the PNS and induces neurite outgrowth in dorsal root ganglia explants.[4,8,9]

No known disease associations exist for *LGI3* (MIM: 608302), but its paralogues *LGI1* (MIM: 604619) and *LGI4* (MIM: 608303) associate with neurological disease traits: familial temporal lobe epilepsy (FTLE [MIM: 600512]) and neurogenic arthrogryposis multiplex congenita 1, with myelin defects (AMC1 [MIM: 617468]), respectively.[10–13] Antibodies against LGI1 can be found in acquired autoimmune limbic encephalitis and peripheral nerve hyperexcitability syndromes (PNHSs).[14,15]

PNHSs are a rare group of neurological disorders characterized by clinical and electrodiagnostic evidence for instability of neurotransmission in lower motor neurons or peripheral motor nerves resulting in spontaneous discharges, such as fasciculations, myokymia, neuromyotonia, and overactivity of the muscle groups, leading to muscle stiffening, cramps, and gait impairment.[14] Occasionally, CNS features such as agitation, memory loss, ataxia, dysarthria, seizures, autonomic dysfunction, dystonia, and/or dyskinesia are observed.[14,16–18] The majority of PNHSs are acquired immune-mediated disorders, including Isaacs syndrome [MIM: 160120], Morvan syndrome, and cramp-fasciculation syndrome.[14]

Evidence for peripheral nerve hyperexcitability is observed in several genetic syndromes, the "genetic PNHSs," such as *KCNA1*-related episodic ataxia type 1 (EA1)/myokymia syndrome (MIM: 160120), *KCNQ2*-related benign familial neonatal epilepsy type 1 and/or myokymia (MIM: 121200), *HINT1*-related neuromyotonia and axonal neuropathy (MIM: 137200), *ADCY5*-related familial dyskinesia with facial myokymia (MIM: 606703), and *PNKD*-related paroxysmal non-kinesigenic dyskinesia 1 (MIM: 118800).

We describe a genetic PNHS due to bi-allelic *LGI3* LoF in 16 subjects from eight unrelated families. Prominent clinical features include global developmental delay (GDD), intellectual disability (ID), facial myokymia, distal deformities, and hyporeflexia/areflexia demonstrating both CNS and PNS dysfunction. Our data in mice and humans suggest a plausible model to explain electrodiagnostic myokymia and the appearance of observable facial myokymia.

Legal guardians of affected individuals provided written informed consent for clinical data sharing, collection and storage of biological samples, experimental analyses, and publication of relevant findings as well as images and videos. The study was performed in agreement with the Declaration of Helsinki and was approved by the relevant institutional ethics committees from participating centers that connected through GeneMatcher.[19] Individual case reports can be found in the supplemental notes. Family 4 was previously included in a gene discovery cohort.[20] Exome sequencing (ES) was implemented with genomic DNA extracted from leukocytes. Sanger di-deoxynucleotide sequencing was performed in all available family members and have validating variant alleles and confirmed their segregation in accordance with Mendelian expectations (supplemental information). We used unphased ES data in families 1, 5, and 6 to determine absence of heterozygosity (AOH) of genomic intervals and infer runs of homozygosity (ROH) representing haplotypes "homozygosed" via identity by descent (IBD) versus identity by state (IBS) and to calculate the estimated coefficient of inbreeding, FROH, for fraction of genome shared (supplemental information). We used ExomeDepth, a tool utilizing read depth from ES data as a surrogate measure of copy-number variants (CNVs), to detect the homozygous multi-exonic intragenic deletion in *LGI3* in family 1.[21] Characterization of the exonic CNV event, breakpoint junctions, and inference of mutational mechanisms is detailed in the supplemental information.

Families originated from multiple countries and diverse ethnic backgrounds (Figure 1A and Table 1). All families reported a history of consanguinity with first-degree-cousin marriage except for two families (family 5A and family 7). Family 5A's parents however were descendants of the same large tribe. The estimated inbreeding co-efficient FROH of their affected children (family 5A, II-1 and II-2) was 0.04 and 0.022, respectively, approaching that of a second-degree-cousin marriage ($F = 0.03125$).

All *LGI3* variants found in these families are listed in Table 1. Identified variants have been deposited to ClinVar (ClinVar: SUB11712385). Alleles include five predicted LoF variants (three frameshift, one nonsense, and one multi-exonic deletion) and two missense variant alleles (Table 1 and Figures 1C and S1; [GenBank: NM_139278.4]). The two intronic +1/−1 variants (8: 22011480, c.494+1G>C and 8: 22006491, c.830 1G>A) are located at a canonical splice site that most likely causes aberrant splicing (SpliceAI highest confidence score (0.99–1.00) on both variants).[22] How such putative splicing defects affect LGI3 protein expression remains to be determined.

The missense variant p.Leu141His localizes to the LRR domain whilst the missense variant p.Asp331Asn

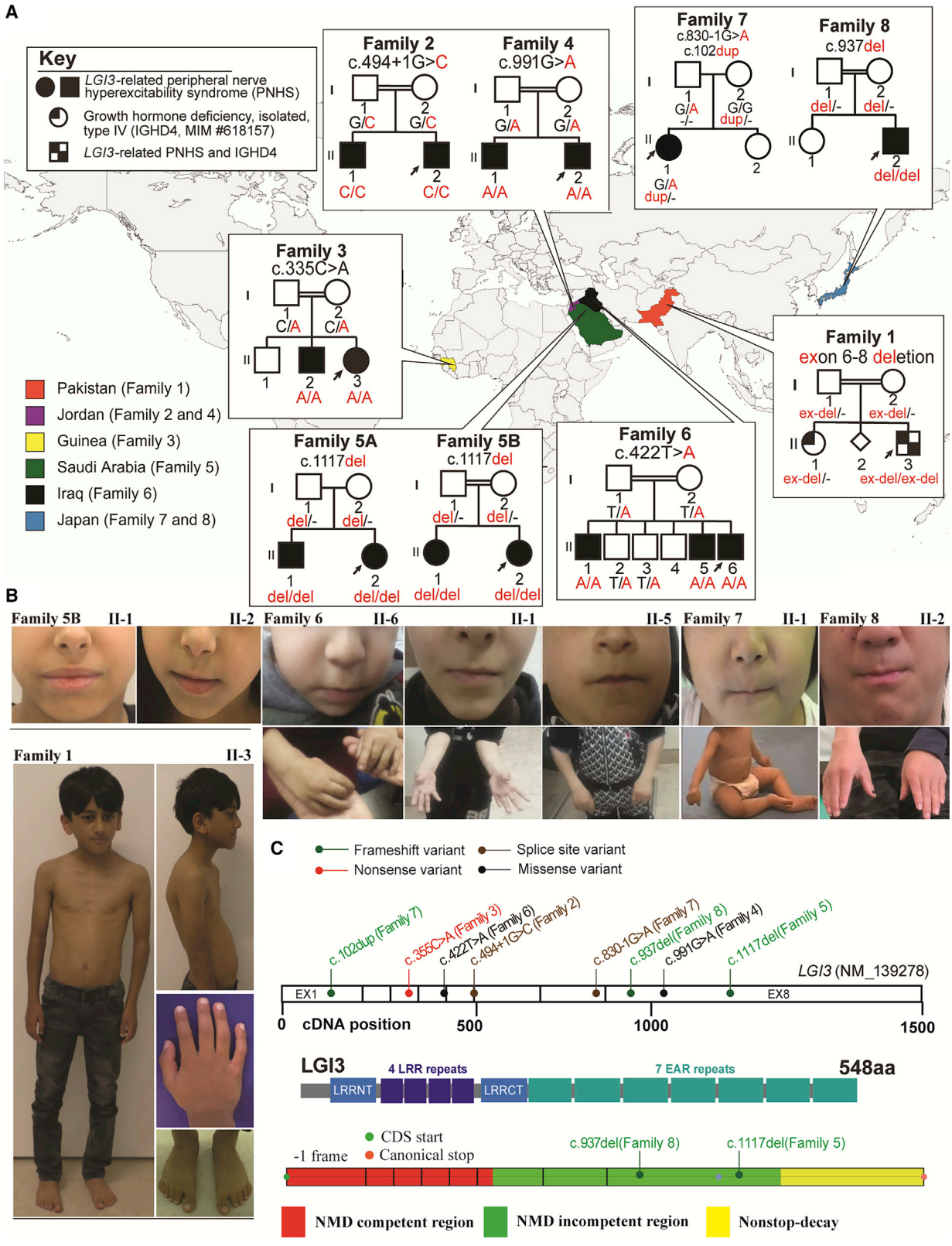

Figure 1. Pedigrees, photographs, and variants' location in the eight families with bi-allelic variants in *LGI3*

(A) A world map showing countries of origin of each family in the study along with their pedigree. The genotype of the variant can be found under each individual in the pedigree.

(B) All available clinical photos of affected individuals with *LGI3*-related disorder in this study are displayed. Note the small mouth (except for family 5B, II-1 and II-2) and distal deformities in the fingers in the affected individuals. Individual II-3 (family 1) also has short stature, thin build, and genu valgum, syndactyly, camptodactyly, and kypholordosis.

(C) A schematic of *LGI3* with the location of the variants across the gene shown. Below the gene structure is the LGI3 protein structure with its different domains including the LRR and EAR repeats.

Table 1. Summary of *LGI3* variant alleles in the eight unrelated families

Family	Country of origin	Consanguinity by history	Position (GRCh37\ hg19)	Nucleotide (protein) (GenBank: NM_139278.4)	dbSNP ref.	Zygosity	Allele count/ zygosity (gnomAD)	CADD score (PHRED)	Conservation, 100 vert, cons. (phyloP100 wayAll)	AOH (around *LGI3*/ total)
Family 1	Pakistan	yes (1° cousins)	del exons 6-8		N/A	hmz	N/A	N/A	N/A	40 Mb/ 330 Mb
Family 2	Jordan	yes (1° cousins)	chr8: 22011480; C>G	c.494+1G>C	rs1827450545	hmz	0 htz–0 hmz	33	7.14961	N/A
Family 3	Guinea	yes (1° cousins)	chr8: 22012088; G>T	c.335C>A (p.Ser112*)	rs769376680	hmz	2 htz–0 hmz	41	4.93405	N/A
Family 4	Jordan	yes (1° cousins)	chr8: 22006329; C>T	c.991G>A; (p.Asp331Asn)	rs1050199719	hmz	1 htz–0 hmz	26.1	4.43004	N/A
Family 5A	Saudi Arabia	no	chr8: 22006203; delA	c.1117del (p.Trp373 Glyfs*18)	N/A	hmz	0 htz–0 hmz	N/A	9.27922	15/265–300 Mb
Family 5B		yes (1° cousins)								2 Mb/ 107–237 Mb
Family 6	Iraq	yes (1° cousins)	chr8: 22011655; A>T	c.422T>A (p.Leu141His)	N/A	hmz	0 htz–0 hmz	33	9.0998	23–28 Mb/ 604–647 Mb
Family 7	Japan	no	chr8: 22006491; C>T (pat)	c.830−1G>A	N/A	comp htz	0 htz–0 hmz	33	7.07505	N/A
			chr8: 22013954; dupG (mat)	c.102dup (p.Lys35G lnfs*86)	Rs749644081		0 htz–0 hmz	N/A	0.132937	N/A
Family 8	Japan	yes (1° cousins)	chr8: 22006383; delT	c.937del (p.Thr313 Argfs*20)	N/A	hmz	1 htz–0 hmz	N/A	0.756417	N/A

Abbreviations: AOH, absence of heterozygosity; CADD, combined annotation-dependent depletion; comp htz, compound heterozygous; hmz, homozygous; htz, heterozygous; mat, maternal inherited; N/A, not available; pat, paternal inherited; ref., reference.

(encoded by c.991G>A) localizes to the EPTP domain. The mutant encoding p.Leu141His variant (c.422T>A) is located 1 bp from the exon-intron junction but is predicted not to affect mRNA splicing (SpliceAI score of 0.00–0.09).[22] Both missense mutations are predicted to be damaging, and we show that indeed the mutant proteins accumulate in the endoplasmic reticulum (ER) and are secreted at severely reduced levels (Figures S1B–S1E). Thus, these mutations represent probable functional-null alleles of *LGI3*. However, it is likely that the clinical phenotype of members of families 4 and 6 is further impacted by ER stress, as production of these mutant proteins results in strong ER accumulation and upregulation of chaperone proteins (Figure S1E–E1).

The deleterious variants in *LGI3* were homozygous and conformed with expected autosomal recessive (AR) trait inheritance in all families except for family 7 with no reported consanguinity or tribal marriage in which the variants were compound heterozygous.

Interestingly, the two branches of family 5 (5A and 5B) were not known to be related but were from the same geographic region and carried the same variant allele that may represent a clan genomics-derived founder allele.[23] Further exploration of extended pedigrees revealed a shared ancestor, and the variant allele was identified within an overlapping AOH block of 1.9 Mb with a total AOH of 107–137 Mb by AOH haplotype analysis of affected children (Figure S2). Note the *LGI3* embedded AOH block of 15 Mb for family 5B with a total AOH of 265–300 Mb (Figure S2). Two subjects carried a second molecular aberration, including chr16q13.11 microduplication of unknown significance (family 7; individual II-1) and pathogenic homozygous variant in *GHRHR* (c.214G>T [p.Glu72*] [GenBank: NM_000823.3]) (family 1, II-3) causing AR isolated growth hormone deficiency type IV (IGHD4 [MIM: 618157]); thus, the multi-locus pathogenic variation in this proband may result genetically by distributive ROH.

A homozygous intragenic deletion involving exons 6 to 8 of *LGI3*, which has eight coding exons, was identified in the proband from family 1 (Figure 2A). Nucleotide-level resolution of the breakpoint junction was obtained and confirmed a homozygous deletion allele (~1.5 kb band) in proband genomic DNA (gDNA), suggesting genomic deletion size of ~6.9 kb; both parents and the unaffected sister were heterozygous carriers of the exonic deletion. In contrast, only the wild-type (WT) allele (~8.4 kb band) was observed in the gDNA control (Figure 2B).

Eight possible CNV-*Alu* pairs were predicted with an AAMR genomic instability risk score of 0.469 for MIM

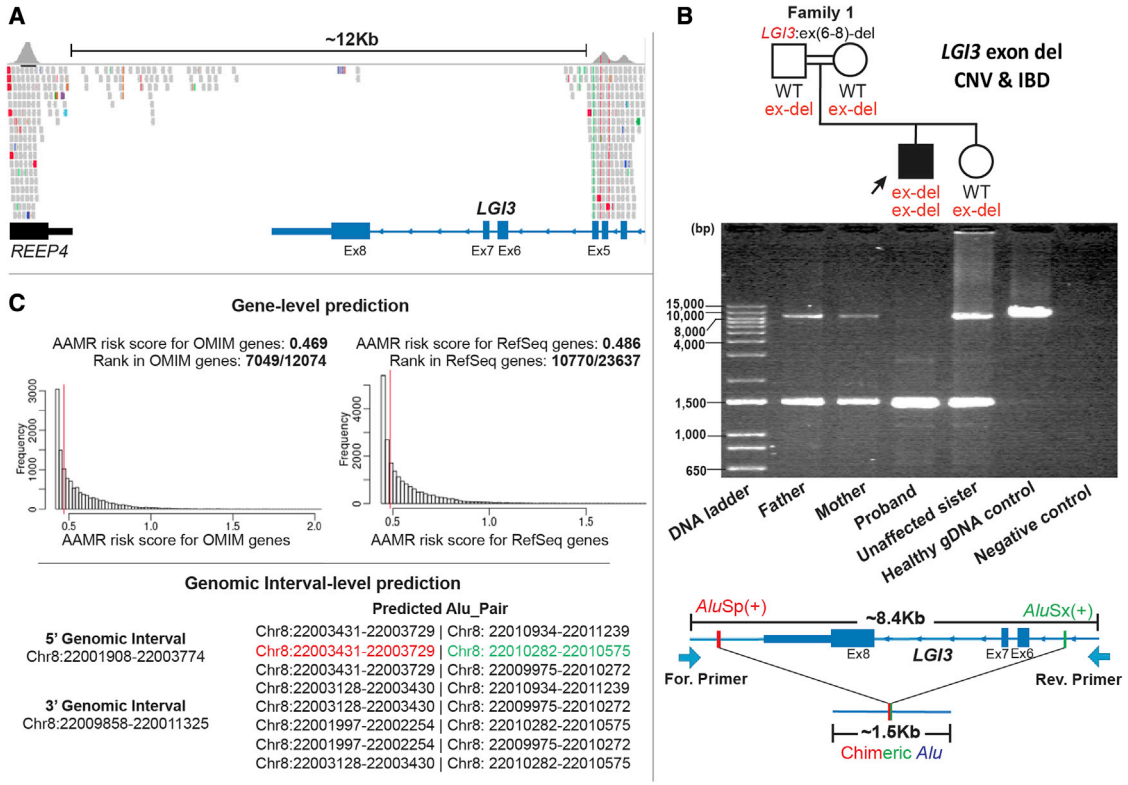

Figure 2. The genomic architecture of the multi-exonic intragenic deletion of *LGI3* in amily 1 derived from an *Alu/Alu*-mediated genomic rearrangement (AAMR)

(A) A screenshot of the proband's exome sequencing data (integrated genomic view [IGV]) showing an approximately 12 kb homozygous intragenic deletion involving exons 6–8 of the exon *LGI3*.

(B) A pedigree of the family 1 followed by the 1% agarose gel electrophoresis of PCR products generated using a primer flanking exon 6–8 in *LGI3* and positioned 8.4 kb apart. From left to right: parents with two bands of ~1.5 kb and ~8.4 kb representing the two alleles at this locus and consistent with the expected sizes for one deleted and one wild-type (WT) non-deleted allele (WT = reference haploid genome); proband with a PCR band of ~1.5 kb consistent with a single deleted allele; unaffected sister with two bands, heterozygous alleles, like parental alleles; healthy gDNA control with one WT non-deleted allele (~8.4 kb band); and negative control (no template). The schematic below the gel shows the genomic profile of *Alu*Sp/*Alu*Sx-pair-mediated rearrangement. The long-range PCR primer pair was designed to produce an amplicon size of ~8.4 kb for WT non-deleted allele and ~1.5 kb for deleted allele resulting from AAMR with formation of a recombinant or chimeric *Alu*.

(C) A screenshot from AluAluCNVPredictor shows gene-level prediction including AAMR risk score of *LGI3* in MIM genes and RefSeq genes. A gene with a risk score higher than 0.6 is considered "at increased relative risk" for genomic instability and susceptibility to AAMR. Genomic interval-level prediction shows eight possible CNV-*Alu* pairs intersecting the given genomic intervals. The specific *Alu*Sp/*Alu*Sx pair that was implicated by experimental data in generating the intragenic deletion in this family is marked with colored font.

genes and 0.486 for RefSeq genes; the latter references haploid human genome computationally annotated genes for *LGI3* (Figure 2C). Examination of the haploid human reference genome showed multiple directly oriented *Alu* elements flanking the deletion region, suggesting potential susceptibility to AAMR (Figure S3A). Sanger sequencing across the breakpoint junction in the deleted allele showed a chimeric, or recombinant, *Alu* element yielded from *Alu*Sp/*Alu*Sx recombination, with 65 bp microhomology at the apparent recombinant joint (Figure S3B) consistent with AAMR's generating the new mutation haplotype in the clan.

Table 2 summarizes the developmental and neurological features of the 16 individuals from eight unrelated families with deleterious bi-allelic *LGI3* variants (further detailed in supplemental notes and Tables S1 and S2). All affected subjects had mild to moderate GDD (16/16), ID (13/13). Prominent neurological features included distal limb deformities (14/16); areflexia or hyporeflexia (10/16); tone abnormalities (7/13) including lower limb hypotonia in three subjects (one also with truncal hypotonia) and peripheral hypertonia/stiffness in five; and near-continuous facial myokymia (7/16) (Video S1) associated with a small mouth with restricted opening (6/16). The facial myokymia was noted as early as 3 months of age (family 6). Distal deformities included knee, hip, and ankle contractures (4/14); contractures/deformities of fingers and feet (6/14); and other uncharacterized deformities (4/14).

Less common features included umbilical or diaphragmatic hernias (4/16), gait abnormality (5/16), neurobehavioral traits including autism spectrum disorder (5/16) or attention deficit hyperactivity disorder (4/16), tongue

Table 2. Developmental and neurological features in the 16 affected individuals with bi-allelic deleterious variants in *LGI3*

	Developmental characteristics				Neurological features						
Individuals	Age at last exam	Sex	GDD	ID	Areflexia/ hyporeflexia	Distal deformities	Facial myokymia	Small mouth with restricted opening	Tongue fasciculations	Abnormal NCS	Myokymia or fasciculations on EMG
Family 1, II-3	7 years	M	+	N/A	+	+	–	–	–	–	N/A
Family 2, II-1	9 years	M	+	N/A	+	+	–	–	–	N/A	+
II-2	6 years	M	+	N/A	+	+	–	–	–	+	+
Family 3, II-2	7 years	M	+	+	+	+	+	+	+	N/A	–
II-3	4 years 7 months	F	+	+	+	+	+	+	+	N/A	+
Family 4, II-1	22 years	M	+	+ (mild)	–	–	–	–	–	N/A	N/A
II-2	20 years	M	+	+ (mild)	–	–	–	–	–	N/A	N/A
Family 5A, II-1	11 years	M	+	+ (mild)	–	+	–	–	–	–	–
II-2	9 years	F	+	+ (mild)	–	+	–	–	–	–	–
Family 5B, II-1	13 years	F	+	+ (mild)	–	+	–	–	–	N/A	N/A
II-2	9 years	F	+	+ (mild)	–	+	–	–	–	N/A	N/A
Family 6, II-1	13 years	M	+	+ (moderate)	+	+	+	+	–	–	N/A
II-5	6 years	M	+	+ (mild)	+	+	+	+	–	–	+
II-6	3 years	M	+	+ (mild)	+	+	+	+	–	N/A	N/A
Family 7, II-1	12 years 10 months	F	+	+ (moderate)	+	+	+	–	–	–	+
Family 8, II-2	13 years	M	+	+ (moderate)	+	+	+	+	+	N/A	N/A
Total	n/a	n/a	16/ 16	13/13	10/16	14/16	7/16	6/16	3/16	1/7	5/8

Abbreviations: EMG, electromyography; F, female; GDD, global developmental delay; ID, intellectual disability; M, male; N/A, not available; n/a, not applicable; NCS, nerve conduction study.
Through the power of human paralog gene studies, worldwide family-based genomics analyses, and mouse studies, we define a potentially recognizable peripheral hyperexcitability syndrome in 16 individuals with bi-allelic *LGI3* variants and show that LGI3 co-localizes with juxtaparanodal voltage-gated potassium channels and its loss results in mis-localization of potassium channel complexes.

fasciculations (3/16), and seizures (2/16). Other rarely observed features—seen only in one subject each—include severe progressive microcephaly (Z score −5 SD), failure to thrive (FTT; weight at −4 SD), short stature (height at −4 SD), growth hormone (GH) deficiency, kyphosis (in family 1, II-3 with IGHD4), bilateral hip dysplasia, *pectus carinatum*, anxiety, eczema, celiac disease, hypokinesia, and ataxia.

Nerve conduction studies (NCSs) were normal in six subjects (6/7) while one subject (1/7) (family 2, II-2) at age 6 years had an abnormal NCS consistent with an axonal neuropathy (supplemental information, Table S2). Myokymic discharges or fasciculations were characteristically observed in the majority (5/8) of those who underwent an EMG study (Figure S4); the discharges were not related to age or variant type. Muscle biopsy was performed in two siblings (family 2) with non-specific findings of increased citrate synthase activity without deficiency in respiratory chain enzymes in the first child and slight denervation atrophy with type 1 fiber "smallness" in some fascicles in the sibling. Brain MRI was normal in most subjects (6/8) and abnormal in two subjects. One subject, with a second molecular diagnosis causing GH deficiency, showed a small hypophysis, whereas the other showed mild frontal hypoplasia. Four subjects underwent routine EEG study, which revealed occasional epileptiform activity in two subjects, one of which has seizures (family 4, II-1).

The myokymic discharges and fasciculations observed in a subset of individuals could result from perturbations to

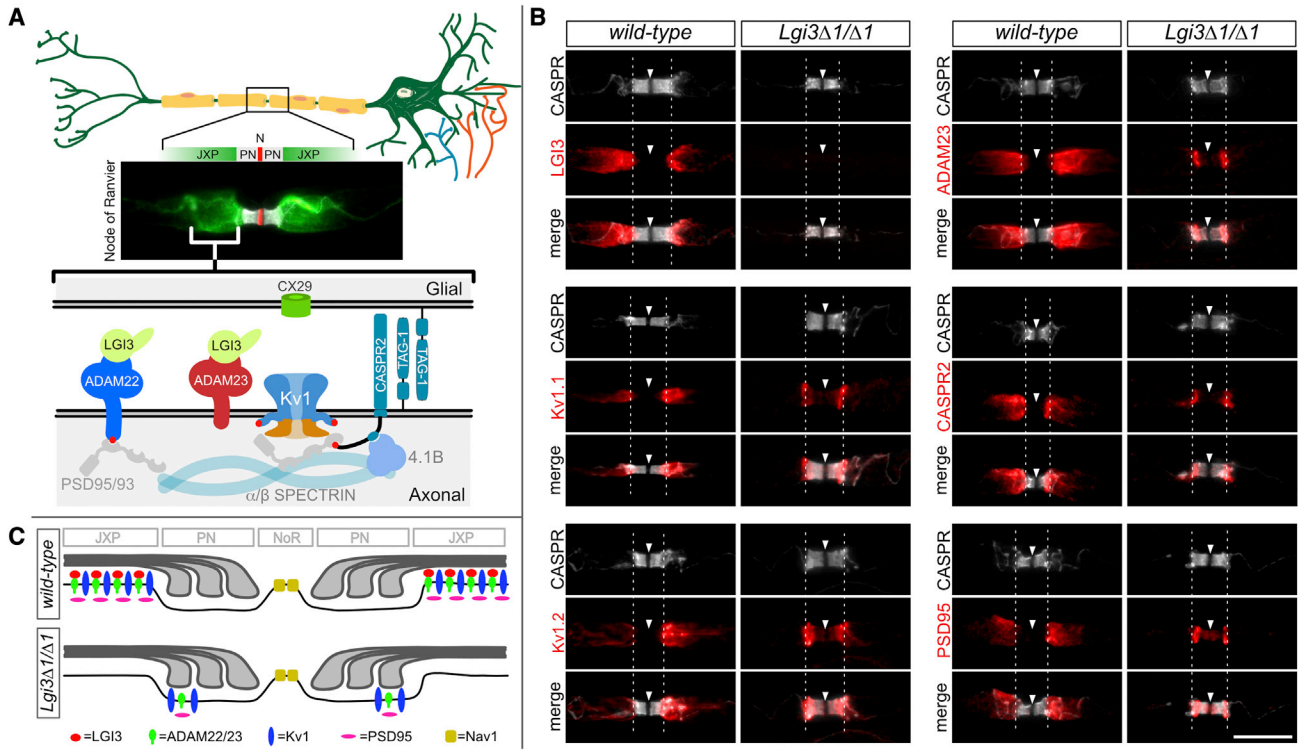

Figure 3. A schematic illustration of the myelinated peripheral nerves, the microanatomy of the nodes of Ranvier

(A) Saltatory conduction in myelinated axons depends on the sequestration of voltage-gated ion channels to the node of Ranvier, the narrow gaps between adjacent myelin sheets. The immune fluorescence image shows the distribution of Kv1 voltage-gated potassium channels (green) under the myelin sheet, in what is referred to as the juxtaparanodal membrane, next to the paranodal junctions (PN in gray) that separate them from the voltage-gated sodium channels Nav1 in the nodal membrane (N in red). At the bottom is a schematic illustration of the juxtaparanodal region highlighting some of the proteins that are highly expressed here. LGI3 binds ADAM23 and/or ADAM22 in the juxtaparanodal membrane. Note that Kv1.1, CASPR2 (CNTNAP2), and TAG-1 (CNTN2) have been implicated in autoimmune peripheral nerve hyperactivity syndrome (PNHS). Additionally, *CASPR2* (MIM: 610042) and *ADAM22* (MIM: 617933) have been implicated in neurodevelopmental disorders and epilepsies and *LGI4* and *CASPR* (also known as *CNTNAP1*) (MIM: 616286), a component of the paranodal junctions, in neurogenic arthrogryposes.

(B) Loss of LGI3 results in reduced and mis-localized Kv1 channel complex in myelinated axons. Representative images of nodes of Ranvier in sciatic nerve axons of 8 week-old WT and *Lgi3* $^{\Delta 1/\Delta 1}$ mice immunolabelled with antibodies against the paranodal protein CASPR (CNTNAP1) (grey) and members of the JXP: LGI3, Kv1.1, Kv1.2, ADAM23, CASPR2 (CNTNAP2), and PSD95 (DLG4) (red). Arrowheads (node) and dashed lines (PN/JXP border) highlight the localization of JXP proteins in the paranode of mutant mice compared to their JXP expression in WT controls. Scale bar: 10 μm.

(C) Graphical representation of the distribution of JXP Kv1 complexes in the presence and absence of LGI3.

the myelinated axons of the facial nerve. We therefore explored whether the LGI3 is present in the myelinated axons of the mouse PNS and what consequence deletion of *Lgi3* has. LGI3 is found at high levels in PNS sensory and motor neurons (Allen Mouse Brain Atlas: https://mouse.brain-map.org/).[4] Within peripheral myelinated axons, LGI3 is highly expressed at the juxtaparanodal membrane, co-localizing with the voltage-gated potassium channels Kv1.1 (KCNA1) and Kv1.2 (KCNA2), associated proteins CASPR2 (CNTNAP2) and PSD95 (DLG4), and the LGI-binding proteins ADAM23 and ADAM22 (Figure 3A and 3B). To assess how loss of LGI3 impacts this organization, we generated homozygous *Lgi3*-null mice (*Lgi3*$^{\Delta 1/\Delta 1}$, Figure S6). *Lgi3* mutant mice are fertile, have a normal lifespan, and do not show obvious behavioral abnormalities. We found that the homozygous deletion of *Lgi3* resulted in strongly reduced expression and mis-localization of Kv1 channel complexes that infringe on the paranodal domain (Figures 3B and 3C). This mis-localization of Kv1 channel complexes is further exacerbated following nerve injury, as Kv1 complexes are confined to the paranodal domain in remyelinated axons (Figure S5). It is speculated that these reduced and mis-localized Kv1 complexes affect the electrophysiological characteristics of the myelinated axons and contribute to the axonal hyperexcitability that underpins the observed myokymia in PNHS subjects homozygous for *LGI3* LoF alleles.

The majority of the subjects had neuropathic features such as distal contractures/deformities (14/16) and diminished reflexes (10/16) despite normal NCSs (6/7). Depressed reflexes have been observed in autoimmune PNHSs.[24] Interestingly, motor and sensory NCSs are often normal in Isaacs syndrome, an autoimmune PNHS, except for after-discharges best observed on repetitive nerve stimulation, which were not performed in any of our

subjects.[24] Additionally, nearly half of our subjects (7/16) had characteristic clinically visible facial myokymia, and the majority of those who underwent EMG (5/8) had findings suggestive of motor nerve hyper-excitability such as myokymia and/or fasciculations. The reason for normal NCS despite the presence of neuropathic features remains to be explored.

Myo-kymia, Greek for "muscle waves," was first reported in the late 1800s independently by two German clinicians, Kny and Schultze.[14,25,26] Facial myokymia, a distinct neurological phenomenon and an exceedingly rare form of myokymia, was described later in 1902 by Bernhardt as "continuous undulant quivering fasciculation of the muscles of the face".[27] In a majority of cases, the myokymia occurs abruptly because of an acquired etiology, specifically pontine glioma and multiple sclerosis, although idiopathic cases have been described.[18,27–29] Myokymia is thought to represent abnormal firing of the motor neuron or peripheral motor nerves.[16] The pathology in facial myokymia is speculated intramedullary in the brainstem and close to the facial nucleus.[27,29] Many subjects also had narrowing of the palpebral fissures, updrawn angle of the mouth, and similar to our subjects, pursing of the lips consistent with the wide involvement of facial musculature as a potential underlying basis of the facial dysmorphology gestalt.[27,29]

Facial myokymia has also been observed in *ADCY5*-related disorder (MIM: 606703) in association with chorea/dyskinesia disorder and in a subject with dominant-negative heterozygous *KCNQ2* mutation with distal contractures and febrile seizures but, in contrast to our subjects, without GDD/ID.[16,18] The visible myokymia in *LGI3*-related disorder is restricted to the face (peri-orbital and peri-oral). Few subjects also had tongue fasciculations and electromyographic myokymia and fasciculations suggesting the involvement of other cranial and peripheral nerves (Table 2 and Table S1). Myokymia, neuromyotonia, and fasciculations can also occur in other genetic PNHSs, such as *HINT1*-, *KCNA1*-, and *PNKD*-related disorders (MIM: 137200, 160120, and 118800, respectively).[30]

The overlap between acquired immune-related and genetic (inherited) disorders is an evolving concept, and exploring myokymia in both acquired and inherited disease can reciprocally inform the mechanism and pathogenesis of both.[31,32] The implication of voltage-gated potassium channels (VGKCs) in both autoimmune and genetic PNHSs is a salient example. Autoimmune PNHSs are occasionally paraneoplastic in origin, and antibodies against VGKC complex are often detected.[14,33] In parallel, mutations in *KCNA1* and *KCNQ2* encoding juxtaparanodal and nodal VGKCs (Kv1.1 and Kv7.2, respectively) associate with myokymia.[17,18] VGKCs dampen neuronal excitability by determining resting action potential, setting threshold for excitation, controlling firing frequency, and promoting repolarization after action potential.[34,35] Suppression of outward VGKCs' current and induced repetitive nerve firing in dorsal root ganglia is observed in subjects with Isaacs syndrome.[36,37]

Notably, anti-VGKC complex antibodies are not solely directed towards VGKCs but often target associated complex-forming proteins such as CASPR2 and CONTACTIN-2 (CNTN2, also called TAG-1), as well as LGI1, although the majority of antigen targets remain unknown (Figure 3).[33] It is thus not surprising to see that impairment of VGKC in the PNS and its interactomes are heavily implicated in PNHSs. Indeed, we demonstrate that loss of LGI3 in mice affects VGKCs and results in strongly reduced and mis-localized expression of Kv1 protein complexes at the juxtaparanodal domain of the node of Ranvier thus likely contributing to the PNHS phenotype (Figure 3). How other genetic PNHS-associated proteins, such as ADCY5 and PNKD, potentially interact with VGKCs remains to be explored. We propose that identifying and describing genetic PNHSs, such as *LGI3*-related disorder, can inform the neurobiology of axonal transmission and illuminate the pathophysiology of immune-related PNHS and potentially define new antigen targets.

Genetic PNHSs have an overlapping organismal phenotype, yet each has unique features in sync with the protein's function and its anatomical and temporal expression. The paroxysmal episodes of ataxia and dysarthria, painful contractures, and myokymia in *KCNA1*-related EA1 are compatible with the Kv1.1 expression in the cerebellum and peripheral nerves.[17,35] *ADCY5* is highly expressed in the striatum correlating with the associated movement disorder phenotype.[16] Furthermore, the Kv7.2 (KCNQ2) peak brain expression at birth and its expression at the nodes of Ranvier and axon initial segment is consistent with the *KCNQ2*-related neonatal seizures and myokymia phenotype.[34,38] Similarly, the CNS and PNS features of this *LGI3*-related disorder align with LGI3's widespread cortical and peripheral nerve expression and role in brain development, neurite growth, and peripheral nerve biology.[7,9,39,40] Interestingly, *LGI3* expression is detected most strongly in the facial nerve nucleus concurring with proposed pathophysiology of facial myokymia.[27,29]

Severe progressive microcephaly (PM), short stature, FTT, GH deficiency, and small hypophysis (as revealed by neuroimaging) were observed in only one individual in this study who also carried a second molecular diagnosis: a *GHRHR* homozygous variant causing IGHD4 (MIM: 618157) that explains the severe growth failure but not the PM. Multi-locus pathogenic variation (MPV) in which variations at two or more genetic loci lead to a blended phenotype accounts for 5% of simplex cases with molecular diagnoses established by clinical exomes and up to 29% of neurodevelopmental disorder (NDD) cases from consanguineous families with increased FROH.[41–43] The individual's total genomic AOH is 330 Mb and consistent with a distributive ROH, raising the possibility for a third contributing locus to explain the PM. Interestingly, one-third of the subjects with NDD from consanguineous families with apparent phenotypic expansion initially attributed to a single known disease-associated gene were later found to have evidence for MPV.[44]

One subject had a multi-exonic intragenic homozygous *LGI3* deletion confirmed experimentally to be mediated by AAMR, an under-recognized mutational mechanism for SV mutagenesis and generation of pathogenic CNV alleles and exonic deletions.[45] Bi-allelic CNVs are increasingly identified as a cause of autosomal recessive traits (AR-CNV) as a result of their increased detection through bioinformatic tools using ES read-depth analyses.[21,46] Surprisingly, the vast majority (~94%) of AR-CNVs affect a single gene, and more than 75% involve a single or only a few exon(s).[46] Small CNVs, such as the one detected in family 1, often arise *de novo* in a common ancestor and become homozygous alleles via IBD.[47] Similarly, the calculated inbreeding coefficient in family 5A (F = 0.22–0.4) and the overlapping AOH interval of 1.9 Mb in available affected children of family 5 (Figure S2) suggest the private variant in both branches (5A and 5B) is most likely a recent clan/tribal allele that arose in a common distant ancestor at least five generations ago.[47]

In summary, a potentially clinically identifiable genetic PNHS was described in 16 individuals with bi-allelic LoF variants in *LGI3*; the clinical synopsis of the disease trait is characterized by GDD/ID, distal deformities with hyporeflexia/areflexia, involvement of facial musculature in the form of small mouth with restricted opening and facial myokymia, and evidence of motor nerve instability on EMG. Mouse studies revealed that LGI3 is highly expressed at the juxtaparanodal membrane and co-localizes with the voltage-gated potassium channels Kv1.1 and Kv1.2 and associated proteins. Moreover, loss of LGI3 results in reduced and mis-localized Kv1 channel complexes in myelinated axons. Human paralogous gene mutational studies and aggregation of worldwide genomic and molecular data, of multiple variant allele types (SNV and CNV), from eight unrelated families with bi-allelic LoF variants in *LGI3* provide insights into (1) clan genomics and (2) organismal nervous system development and function and (3), with mouse investigations, informs the genesis of electrodiagnostic and clinically observed facial myokymia. Paralogous gene studies may also provide a route to molecular therapies.

Data and code availability

This study did not generate any codes or analyze any datasets. Identified variants have been deposited to ClinVar (ClinVar: SCV002558740 and ClinVar: SCV002558748).

Supplemental information

Supplemental information can be found online at https://doi.org/10.1016/j.ajhg.2022.07.006.

Acknowledgments

We thank the families for their participation in the study. M. Jaegle, A. Aunin, and S. Driegen are thanked for generation of the *Lgi3* knock-out mouse line. This study was supported by the U.S. National Human Genome Research Institute and National Heart, Lung, and Blood Institute to the Baylor-Hopkins Center for Mendelian Genomics (BHCMG, UM1 HG006542), NHGRI Baylor College of Medicine Genomics Research Elucidates Genetics of Rare (BCM-GREGoR; U01 HG011758), U.S. National Institute of Neurological Disorders and Stroke (NINDS) (R35NS105078), National Institute of General Medical Sciences (NIGMS, R01GM 106373), the Muscular Dystrophy Association (MDA; 512848), and Spastic Paraplegia Foundation to J.R.L. D.M. was supported by a Medical Genetics Research Fellowship Program through the United States National Institutes of Health (T32 GM007526-42). J.E.P. was supported by NHGRI K08 HG008986. This study was also supported in part by the JSPS KAKENHI (grant number JP20K07907 to S.M.) and the Japan Agency for Medical Research and Development under grant numbers JP21ek0109486, JP21ek0109549, JP21cm0106503, and JP21ek0109493 to N.M. D.P. is supported by International Rett Syndrome Foundation (IRSF grant #3701-1). D.G.C. is supported by NIH Brain Disorder and Development training grant (T32 NS043124-19) and Muscular Dystrophy Association Development grant (873841). T.F. was funded by Philadelphia University, Amman, Jordan. E.A.F. was funded by King Fahad Medical City Research Centre/IRF 019-052. N.K., S.B., and D. Meijer were supported by the UKRI Biotechnology and Biological Sciences Research Council (BBSRC) grant number BB/N015142/1 (to D. Meijer), grant number BB/T00875X/1 (S.B.), and grant number BB/M010996/1 (N.K.).

Declaration of interests

J.R.L. has stock ownership in 23andMe; is a paid consultant for Regeneron Genetics Center; and is a co-inventor on multiple United States and European patents related to molecular diagnostics for inherited neuropathies, eye diseases, genomic disorders, and bacterial genomic fingerprinting. The Department of Molecular and Human Genetics at Baylor College of Medicine receives revenue from clinical genetic testing conducted at Baylor Genetics (BG); J.R.L. serves on the Scientific Advisory Board (SAB) of BG.

Received: March 27, 2022
Accepted: July 1, 2022
Published: August 9, 2022

Web resources

*AluAlu*CNVPredictor, http://alualucnvpredictor.research.bcm.edu:3838/

ExomeDepth, https://github.com/vplagnol/ExomeDepth

GeneMatcher Browser, https://genematcher.org/

gnomAD Browser, https://gnomad.broadinstitute.org/

NMDEscPredictor, https://nmdprediction.shinyapps.io/nmdescpredictor/

Online Mendelian Inheritance in Man, https://www.omim.org/

SpliceAI, https://spliceailookup.broadinstitute.org/

UCSC Genome Browser, https://genome.ucsc.edu

XHMM, http://atgu.mgh.harvard.edu/xhmm/index.shtml

References

1. Kegel, L., Aunin, E., Meijer, D., and Bermingham, J.R. (2013). LGI proteins in the nervous system. ASN Neuro *5*, 167–181.

2. Staub, E., Pérez-Tur, J., Siebert, R., Nobile, C., Moschonas, N.K., Deloukas, P., and Hinzmann, B. (2002). The novel EPTP repeat defines a superfamily of proteins implicated in epileptic disorders. Trends Biochem. Sci. *27*, 441–444.
3. Herranz-Pérez, V., Olucha-Bordonau, F.E., Morante-Redolat, J.M., and Pérez-Tur, J. (2010). Regional distribution of the leucine-rich glioma inactivated (*LGI*) gene family transcripts in the adult mouse brain. Brain Res. *1307*, 177–194.
4. Bermingham, J.R., Jr., Shearin, H., Pennington, J., O'Moore, J., Jaegle, M., Driegen, S., van Zon, A., Darbas, A., Ozkaynak, E., Ryu, E.J., et al. (2006). The claw paw mutation reveals a role for Lgi4 in peripheral nerve development. Nat. Neurosci. *9*, 76–84.
5. Park, W.J., Lee, S.E., Kwon, N.S., Baek, K.J., Kim, D.S., and Yun, H.Y. (2008). Leucine-rich glioma inactivated 3 associates with syntaxin 1. Neurosci. Lett. *444*, 240–244.
6. Okabayashi, S., and Kimura, N. (2008). Leucine-rich glioma inactivated 3 is involved in amyloid beta peptide uptake by astrocytes and endocytosis itself. Neuroreport *19*, 1175–1179.
7. Lee, S.E., Lee, A.Y., Park, W.J., Jun, D.H., Kwon, N.S., Baek, K.J., et al. (2006). Mouse *Lgi3* gene: expression in brain and promoter analysis. Gene *372*, 8–17.
8. Diehn, M., Sherlock, G., Binkley, G., Jin, H., Matese, J.C., Hernandez-Boussard, T., Rees, C.A., Cherry, J.M., Botstein, D., Brown, P.O., and Alizadeh, A.A. (2003). SOURCE: a unified genomic resource of functional annotations, ontologies, and gene expression data. Nucleic Acids Res. *31*, 219–223.
9. Park, W.J., Lim, Y.Y., Kwon, N.S., Baek, K.J., Kim, D.S., and Yun, H.Y. (2010). Leucine-rich glioma inactivated 3 induces neurite outgrowth through Akt and focal adhesion kinase. Neurochem. Res. *35*, 789–796.
10. Ottman, R., Winawer, M.R., Kalachikov, S., Barker-Cummings, C., Gilliam, T.C., Pedley, T.A., and Hauser, W.A. (2004). *LGI1* mutations in autosomal dominant partial epilepsy with auditory features. Neurology *62*, 1120–1126.
11. Xue, S., Maluenda, J., Marguet, F., Shboul, M., Quevarec, L., Bonnard, C., Ng, A.Y.J., Tohari, S., Tan, T.T., Kong, M.K., et al. (2017). Loss-of-Function mutations in *LGI4*, a secreted ligand involved in schwann cell myelination, are responsible for arthrogryposis multiplex congenita. Am. J. Hum. Genet. *100*, 659–665.
12. Kalachikov, S., Evgrafov, O., Ross, B., Winawer, M., Barker-Cummings, C., Martinelli Boneschi, F., et al. (2002). Mutations in *LGI1* cause autosomal-dominant partial epilepsy with auditory features. Nat. Genet. *30*, 335–341.
13. Morante-Redolat, J.M., Gorostidi-Pagola, A., Piquer-Sirerol, S., Sáenz, A., Poza, J.J., Galán, J., et al. (2002). Mutations in the *LGI1/Epitempin* gene on 10q24 cause autosomal dominant lateral temporal epilepsy. Hum. Mol. Genet. *11*, 1119–1128.
14. Sawlani, K., and Katirji, B. (2017). Peripheral nerve hyperexcitability syndromes. Continuum *23*, 1437–1450.
15. Uy, C.E., Binks, S., and Irani, S.R. (2021). Autoimmune encephalitis: clinical spectrum and management. Pract. Neurol. *21*, 412–423.
16. Chen, Y.Z., Matsushita, M.M., Robertson, P., Rieder, M., Girirajan, S., Antonacci, F., et al. (2012). Autosomal dominant familial dyskinesia and facial myokymia: single exome sequencing identifies a mutation in *adenylyl cyclase 5*. Arch. Neurol. *69*, 630–635.
17. Browne, D.L., Gancher, S.T., Nutt, J.G., Brunt, E.R., Smith, E.A., Kramer, P., and Litt, M. (1994). Episodic ataxia/myokymia syndrome is associated with point mutations in the human potassium channel gene. Nat. Genet. *8*, 136–140.
18. Camelo, C.G., Silva, A.M.S., Moreno, C.A.M., Matsui-Júnior, C., Heise, C.O., Pedroso, J.L., and Zanoteli, E. (2020). Facial myokymia in inherited peripheral nerve hyperexcitability syndrome. Pract. Neurol. *20*, 253–255.
19. Wohler, E., Martin, R., Griffith, S., Rodrigues, E.D.S., Antonescu, C., Posey, J.E., Coban-Akdemir, Z., Jhangiani, S.N., Doheny, K.F., Lupski, J.R., et al. (2021). PhenoDB, GeneMatcher and VariantMatcher, tools for analysis and sharing of sequence data. Orphanet J. Rare Dis. *16*, 365.
20. Froukh, T.J. (2017). Next generation sequencing and genome-wide genotyping identify the genetic causes of intellectual disability in ten consanguineous families from Jordan. Tohoku J. Exp. Med. *243*, 297–309.
21. Plagnol, V., Curtis, J., Epstein, M., Mok, K.Y., Stebbings, E., Grigoriadou, S., Wood, N.W., Hambleton, S., Burns, S.O., Thrasher, A.J., et al. (2012). A robust model for read count data in exome sequencing experiments and implications for copy number variant calling. Bioinformatics *28*, 2747–2754.
22. Jaganathan, K., Kyriazopoulou Panagiotopoulou, S., McRae, J.F., Darbandi, S.F., Knowles, D., Li, Y.I., Kosmicki, J.A., Arbelaez, J., Cui, W., Schwartz, G.B., et al. (2019). Predicting splicing from primary sequence with deep learning. Cell *176*, 535–548.e24.
23. Gonzaga-Jauregui, C., Yesil, G., Nistala, H., Gezdirici, A., Bayram, Y., Nannuru, K.C., Pehlivan, D., Yuan, B., Jimenez, J., Sahin, Y., et al. (2020). Functional biology of the Steel syndrome founder allele and evidence for clan genomics derivation of *COL27A1* pathogenic alleles worldwide. Eur. J. Hum. Genet. *28*, 1243–1264.
24. Ahmed, A., and Simmons, Z. (2015). Isaacs syndrome: a review. Muscle Nerve *52*, 5–12.
25. Kny, E. (1888). Ueber ein dem paramyoclonus multiplex (Friedreich) nahestehendes Krankheitsbild. Archiv f. Psychiatrie *19*, 577–590.
26. Schultze, F. (1895). Beitrage zur Musckelpathologie (Deutsch Ztschr f Nervenh), pp. 65–75.
27. Andermann, F., Cosgrove, J.B.R., Lloyd-Smith, D.L., Gloor, P., and Mcnaughton, F.L. (1961). Facial myokymia in multiple sclerosis. Brain *84*, 31–44.
28. Radü, E.W., Skorpil, V., and Kaeser, H.E. (1975). Facial myokymia. Eur. Neurol. *13*, 499–512.
29. Matthews, W.B. (1966). Facial myokymia. J. Neurol. Neurosurg. Psychiatry *29*, 35–39.
30. Amberger, J.S., Bocchini, C.A., Schiettecatte, F., Scott, A.F., and Hamosh, A. (2015). OMIM.org: online Mendelian Inheritance in Man (OMIM®), an online catalog of human genes and genetic disorders. Nucleic Acids Res. *43*, D789–D798.
31. Satoh, M., Ceribelli, A., and Chan, E.K.L. (2012). Common pathways of autoimmune inflammatory myopathies and genetic neuromuscular disorders. Clin. Rev. Allergy Immunol. *42*, 16–25.
32. Vincent, A., Beeson, D., and Lang, B. (2000). Molecular targets for autoimmune and genetic disorders of neuromuscular transmission. Eur. J. Biochem. *267*, 6717–6728.
33. Irani, S.R., Alexander, S., Waters, P., Kleopa, K.A., Pettingill, P., Zuliani, L., Peles, E., Buckley, C., Lang, B., and Vincent, A. (2010). Antibodies to Kv1 potassium channel-complex proteins leucine-rich, glioma inactivated 1 protein and contactin-associated protein-2 in limbic encephalitis, Morvan's

syndrome and acquired neuromyotonia. Brain *133*, 2734–2748.
34. Kole, M.H., and Cooper, E.C. (2014). Axonal Kv7.2/7.3 channels: caught in the act. Channels *8*, 288–289.
35. D'Adamo, M.C., Liantonio, A., Rolland, J.F., Pessia, M., and Imbrici, P. (2020). Kv1.1 channelopathies: pathophysiological mechanisms and therapeutic approaches. Int. J. Mol. Sci. *21*, E2935.
36. Sonoda, Y., Arimura, K., Kurono, A., Suehara, M., Kameyama, M., Minato, S., Hayashi, A., and Osame, M. (1996). Serum of Isaacs' syndrome suppresses potassium channels in PC-12 cell lines. Muscle Nerve *19*, 1439–1446.
37. Shillito, P., Molenaar, P.C., Vincent, A., Leys, K., Zheng, W., van den Berg, R.J., Plomp, J.J., van Kempen, G.T., Chauplannaz, G., Wintzen, A.R., et al. (1995). Acquired neuromyotonia: evidence for autoantibodies directed against K+ channels of peripheral nerves. Ann. Neurol. *38*, 714–722.
38. Kanaumi, T., Takashima, S., Iwasaki, H., Itoh, M., Mitsudome, A., and Hirose, S. (2008). Developmental changes in *KCNQ2* and *KCNQ3* expression in human brain: possible contribution to the age-dependent etiology of benign familial neonatal convulsions. Brain Dev. *30*, 362–369.
39. Okabayashi, S., and Kimura, N. (2007). Immunohistochemical and biochemical analyses of LGI3 in monkey brain: LGI3 accumulates in aged monkey brains. Cell. Mol. Neurobiol. *27*, 819–830.
40. Ozkaynak, E., Abello, G., Jaegle, M., van Berge, L., Hamer, D., Kegel, L., Driegen, S., Sagane, K., Bermingham, J.R., Jr., and Meijer, D. (2010). Adam22 is a major neuronal receptor for Lgi4-mediated Schwann cell signaling. J. Neurosci. *30*, 3857–3864.
41. Posey, J.E., Harel, T., Liu, P., Rosenfeld, J.A., James, R.A., Coban Akdemir, Z.H., Walkiewicz, M., Bi, W., Xiao, R., Ding, Y., et al. (2017). Resolution of disease phenotypes resulting from multilocus genomic variation. N. Engl. J. Med. *376*, 21–31.
42. Pehlivan, D., Bayram, Y., Gunes, N., Coban Akdemir, Z., Shukla, A., Bierhals, T., Tabakci, B., Sahin, Y., Gezdirici, A., Fatih, J.M., et al. (2019). The genomics of arthrogryposis, a complex trait: candidate genes and further evidence for oligogenic inheritance. Am. J. Hum. Genet. *105*, 132–150.
43. Mitani, T., Isikay, S., Gezdirici, A., Gulec, E.Y., Punetha, J., Fatih, J.M., Herman, I., Tayfun, G.A., Du, H., Calame, D., et al. (2021). Evidence for a higher prevalence of oligogenic inheritance in neurodevelopmental disorders in the Turkish population. Am. J. Hum. Genet. *108*, 1981–2005.
44. Karaca, E., Posey, J.E., Coban Akdemir, Z., Pehlivan, D., Harel, T., Jhangiani, S.N., Bayram, Y., Song, X., Bahrambeigi, V., Yuregir, O.O., et al. (2018). Phenotypic expansion illuminates multilocus pathogenic variation. Genet. Med. *20*, 1528–1537.
45. Song, X., Beck, C.R., Du, R., Campbell, I.M., Coban-Akdemir, Z., Gu, S., Breman, A.M., Stankiewicz, P., Ira, G., Shaw, C.A., and Lupski, J.R. (2018). Predicting human genes susceptible to genomic instability associated with *Alu/Alu*-mediated rearrangements. Genome Res. *28*, 1228–1242.
46. Yuan, B., Wang, L., Liu, P., Shaw, C., Dai, H., Cooper, L., Zhu, W., Anderson, S.A., Meng, L., Wang, X., et al. (2020). CNVs cause autosomal recessive genetic diseases with or without involvement of SNV/indels. Genet. Med. *22*, 1633–1641.
47. Lupski, J.R., Belmont, J.W., Boerwinkle, E., and Gibbs, R.A. (2011). Clan genomics and the complex architecture of human disease. Cell *147*, 32–43.